Tectonophysics 824 (2022) 229225

Contents lists available at ScienceDirect

Tectonophysics

journal homepage: www.elsevier.com/locate/tecto

The North-East Atlantic Mid-Norwegian rifted margin: Insights from the deep imaging Geoex MCG RDI19 dataset

Gwenn Peron-Pinvidic [a,b,*], Tor Åkermoen [c], Lars Ivar Leivestad [c]

[a] NGU Geological Survey of Norway, Leiv Eirikssons vei 39, 7040 Trondheim, Norway
[b] Norwegian University of Science and Technology (NTNU), 7491 Trondheim, Norway
[c] Geoex MCG, Norway

ARTICLE INFO

Keywords:
Rifting
Rifted margin
North-East Atlantic
Mid-Norwegian margin
Long-offset
Deep penetrating seismic reflection

ABSTRACT

The Norwegian Continental Shelf is one of the world's most used laboratories to study rifting processes and rifted margin architecture. Available datasets are dense, various and of good quality. However, since the full basement is rarely imaged, major questions remain unanswered regarding the structural details and nature of rocks at depth. The Geoex MCG Regional Deep Imaging 2019 (RDI19) dataset presents - for the first time - a series of regional long-offset seismic reflection profiles, of high resolution and deep imaging (16 s-twtt). The dataset offers an unprecedented imaging of the entire margin architecture including deep basement units, Moho and upper mantle - from the proximal margin to the outer margin.

This contribution introduces the dataset and proposes an interpretation accompanied by gravity modelling experiments. Focus is set on the identification and seismic facies characteristics of the top basement and Moho core envelopes to discuss the dip and lateral variability of the various basement/crustal units. Basic gravity models are used to develop a discussion on the possible nature of the acoustic basement in the distal margin (crust, magma, mantle, combinations). Based on the observations and interpretation, an updated map of the Møre and Vøring margin structural domains is proposed and discussed.

1. Introduction

Møre and Vøring represent the main segments of the Mid Norwegian margin, which lie conjugate to the Jan Mayen microcontinent and southern NE Greenland margin, respectively (Fig. 1). Located in the northern part of the Northeast Atlantic, the rift system has a very long geological history including, for the most recent tectonic events, an orogeny, an orogenic collapse and a rifting. The rift period included several distinct phases of active extension alternating with tectonic pauses, spanning more than 250 Myrs and leading to the formation of a wide sediment rich rifted margin (Blystad et al., 1995; Brekke, 2000; Faleide et al., 2008; Færseth, 2020).

Presenting high oil and gas potential, the Norwegian Continental Shelf has been highly investigated. The available data include numerous wells, seismic reflection, seismic refraction and various other geophysical datasets of high resolution and high quality. The Geoex MCG Regional Deep Imaging 2019 (RDI19) dataset presents a regional coverage of the Møre and Vøring Mid Norwegian margins with deep penetrating 16 s-twtt (seconds two-way travel time) seismic reflection profiles (Fig. 1). The dataset is a unique, unprecedented high-resolution dataset that images - for the first time - the entire basement and sedimentary units at the regional scale, from the most proximal settings to the continent-ocean boundary. The three core boundaries/envelopes (seafloor, top basement, and Moho) - whose identification is necessary to calibrate any interpretation or modelling exercise - can be mapped and studied in a consistent and coherent analysis protocol over the entire rift system, including the proximal domain. Fig. 2 presents three profiles selected as representative of the architecture of the Norwegian Continental Shelf, and of the lateral structural variations from the Møre (profile A) to the Vøring segments (Profiles B and C) (see location on Fig. 1). The profiles are displayed without interpretation above, with a thin white horizontal line at 10 s-twtt illustrating the depth at which most of the available datasets in the region terminate. This demonstrates spectacularly the uniqueness and usefulness of the RDI19 dataset in imaging the entire basement/crustal geometry of the rifted margin. At the bottom, Figures 2abc show the mapping of the core envelopes identifiable on the profiles, including the seafloor, top of acoustic basement and Moho (see below for explanations).

* Corresponding author at: NGU Geological Survey of Norway, Leiv Eirikssons vei 39, 7040 Trondheim, Norway.
E-mail address: gwenn@ngu.no (G. Peron-Pinvidic).

https://doi.org/10.1016/j.tecto.2022.229225
Received 6 September 2021; Received in revised form 7 January 2022; Accepted 10 January 2022
Available online 19 January 2022

Although the Mid Norwegian rifted margin is amongst the best imaged extensional settings in the world, debates remain on e.g., the actual architecture of the sedimentary units at depth and on the composition of the basement in the deep margin. The interpretations proposed in the literature are mostly based on seismic reflection structural mapping and potential field modelling (e.g., Faleide et al., 2010; Osmundsen et al., 2002; Osmundsen and Ebbing, 2008; Fazlikhani et al., 2017; Færseth, 2020). However, in the absence of direct rock sampling, these interpretations remain non-unique and open for discussions. In that context, the Geoex MCG RDI19 dataset is very interesting because it offers an unprecedented imaging of the whole margin and contributes to augmenting our catalogue of observations, which may help progress our discussions towards converging interpretations.

This contribution aims at introducing the Geoex MCG RDI19 dataset, taking advantage of its exceptional imaging to discuss the seismic facies and geometrical characteristics of the top basement and Moho envelopes at the margin scale. We focus on the margin domains, basement units, and their dip and lateral variations. Below we first summarize the geological context of the Møre and Vøring rifted margins. We then briefly present the acquisition and processing characteristics of the dataset. Based on this, we describe the main characteristics of the core envelopes and main acoustic basement units, and use the information, together with some gravity modelling to propose some profile interpretations and an updated map of the margin structural domains.

2. Geological settings

The NE Greenland - Mid Norway rift system, responsible for the formation of the Møre and Vøring margin segments, has a very long extensional history (Brekke, 2000; Faleide et al., 2008; Færseth, 2020). The first rift episodes of rift-related extension are recognized to date from Permian times and the breakup commonly accepted for the Møre and Vøring margin segments is interpreted to occur during Eocene time (Tsikalas et al., 2012). Thus, the rifting history extends over more than 200 Myrs, with a succession of different extensional episodes and phases of apparent tectonic quiescence (Peron-Pinvidic and Osmundsen, 2018). However, the extensional history of the region is more important than any sole rift stage as it also includes an orogenic collapse before the actual beginning of the rifting history (Fossen, 2010). In the south-western parts of onshore Norway, Fossen (2000) reported reversal of movement along orogenic thrusts to accommodate the collapse of the Scandinavian orogen from 405 Ma (Early Devonian). Additionally, it has been recently proposed that rifting *s.s.* may initiate earlier than the Permian period, probably by mid Carboniferous times, by reactivation of

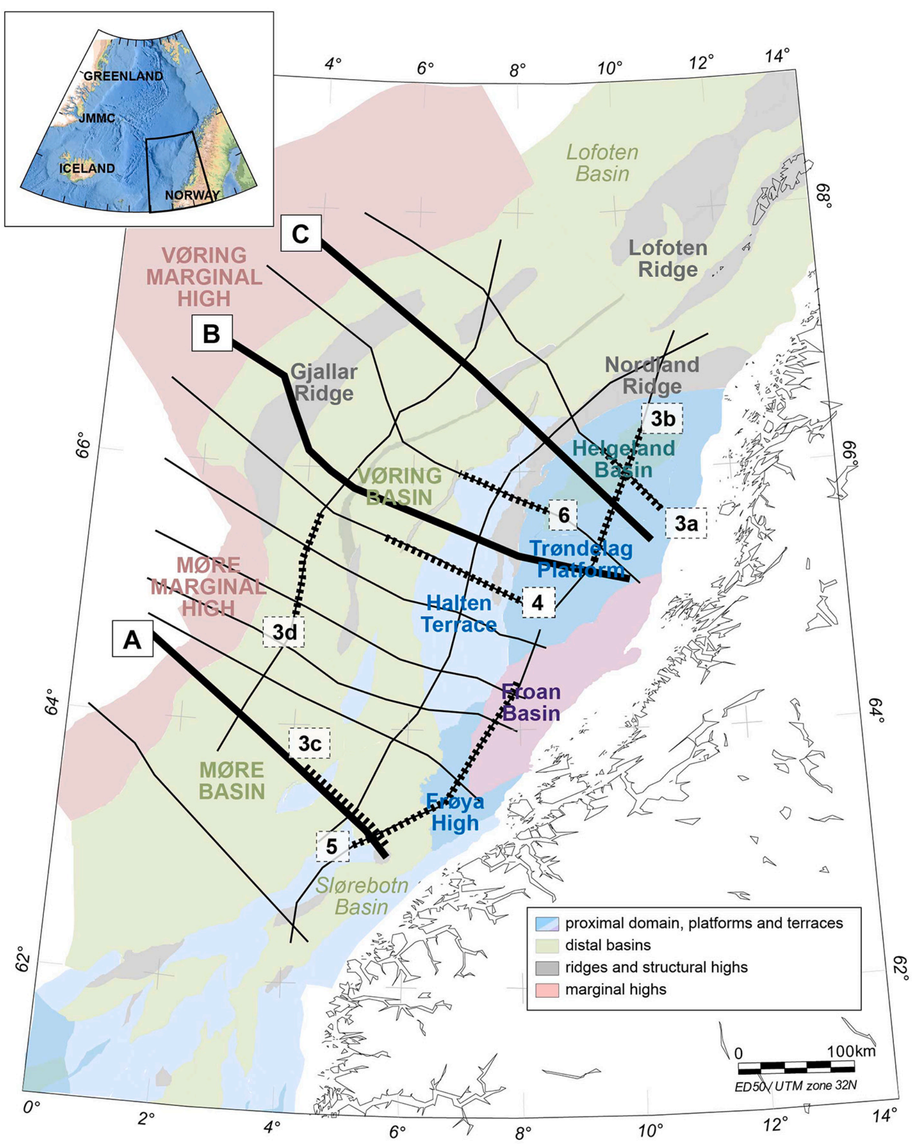

Fig. 1. Structural map of the Mid-Norwegian offshore region discussed in the contribution, with the outline of the main structural elements proposed by the NPD (Norwegian Petroleum Directorate) (after Blystad et al., 1995) - see colour code at bottom right. The black lines show the location of the seismic reflection profiles of the Geoex MCG RDI19 dataset studied in this project. The thick black segments locate the key profiles selected as representative of the architecture of the margin, presented in Figures 2abc. The dashed black segments locate the seismic extracts presented in the other figures. The inset at top left locates the study area within the northeast Atlantic region, with the Jan Mayen microcontinent (JMMC) and NE Greenland margin as conjugates.

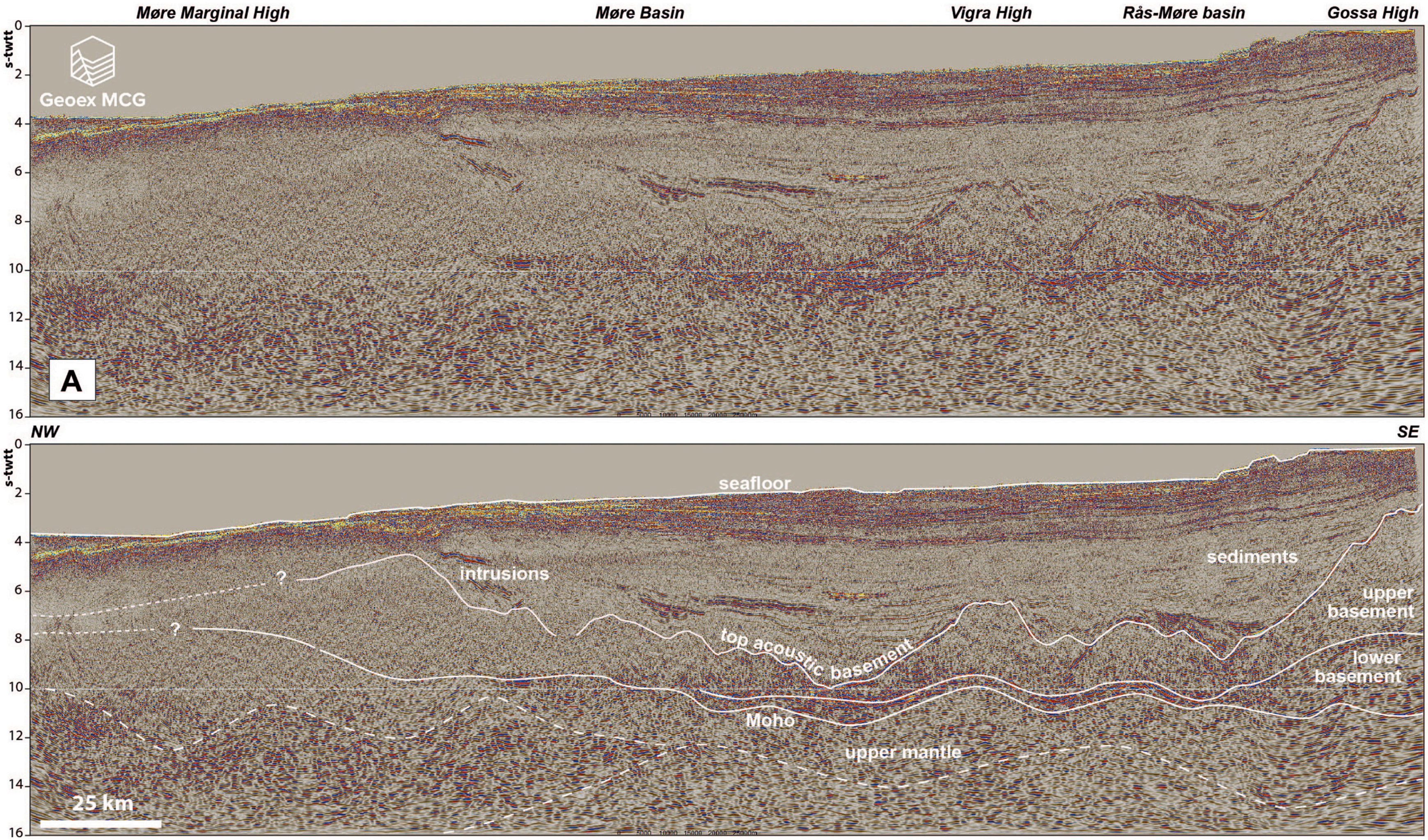

Fig. 2. The three seismic reflection profiles selected in the Geoex MCG RDI19 dataset to illustrate the architecture of the Møre and Vøring segments of the Mid Norwegian margin. 2a. profile A. 2b. profile B. 2c. profile C. The figures illustrate the definition of the core envelopes (seafloor, top acoustic basement and Moho) used as the bases for the interpretation of the regional dataset. See Fig. 1 for location. The horizontal white thin line shows the 10 s-twtt (seconds two-way travel time) as a visual marker to illustrate where the majority of the seismic reflection profiles available in the region stop. Note the advantage of the present dataset to image numerous geometries and seismic facies changes that are located below this 10 s-twtt line. See text for description and analysis.

Tectonophysics 824 (2022) 229225

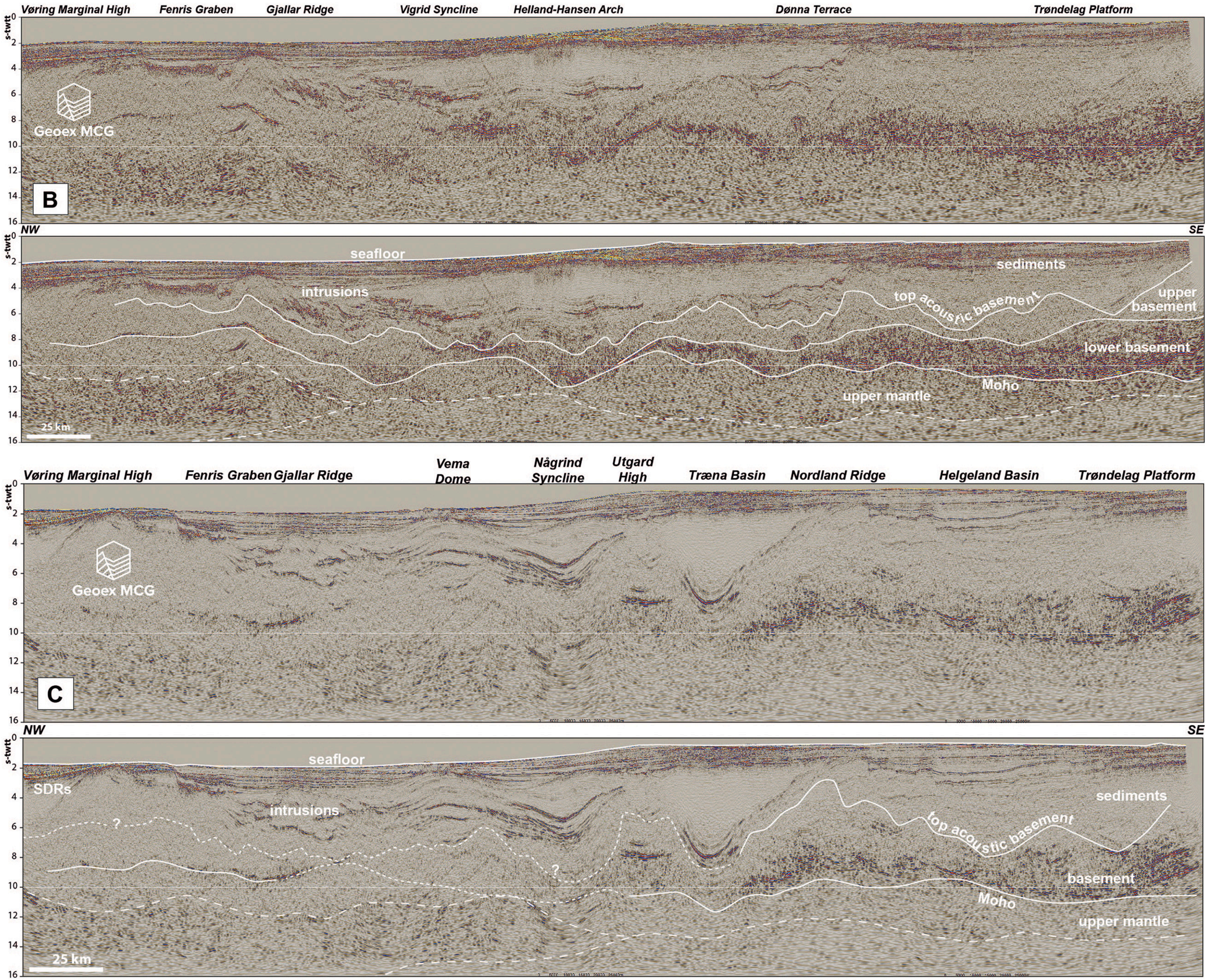

Fig. 2. (*continued*).

some specific tectonic structures (shear zones, detachment faults, core complexes) developed at the collapse stage (Osmundsen et al., 2020; Peron-Pinvidic and Osmundsen, 2020; Peron-Pinvidic et al., 2020). Thus, the extensional history of the Norwegian Continental Shelf is long, composite and multiphase. With the margin being furthermore sediment rich and affected by a significant magmatic phase, the geometries to be studied can present a high level of architectural complexity.

Structurally, the Møre and Vøring margin segments are usually summarized based on the Blystad et al. (1995) 'NPD map' (NPD for Norwegian Petroleum Directorate - the Norwegian government agency responsible for the regulation of the petroleum resources on the Norwegian Continental Shelf) (Fig. 1). Structurally, the margins include, from the SE to the NW: a proximal margin with a platform type environment (the bluish / dark green / purple colours on Fig. 1), which is a domain supposedly developed over a relatively thick basement; a distal margin (light green colours on Fig. 1) with wide basins presenting potentially important thicknesses of sediments over thinned basement; and an outer margin usually summarized as a combination of structural ridges and subbasins with an oceanwards increase in magmatic content in the form of intrusions, extrusions and underplatings (Brekke, 2000;

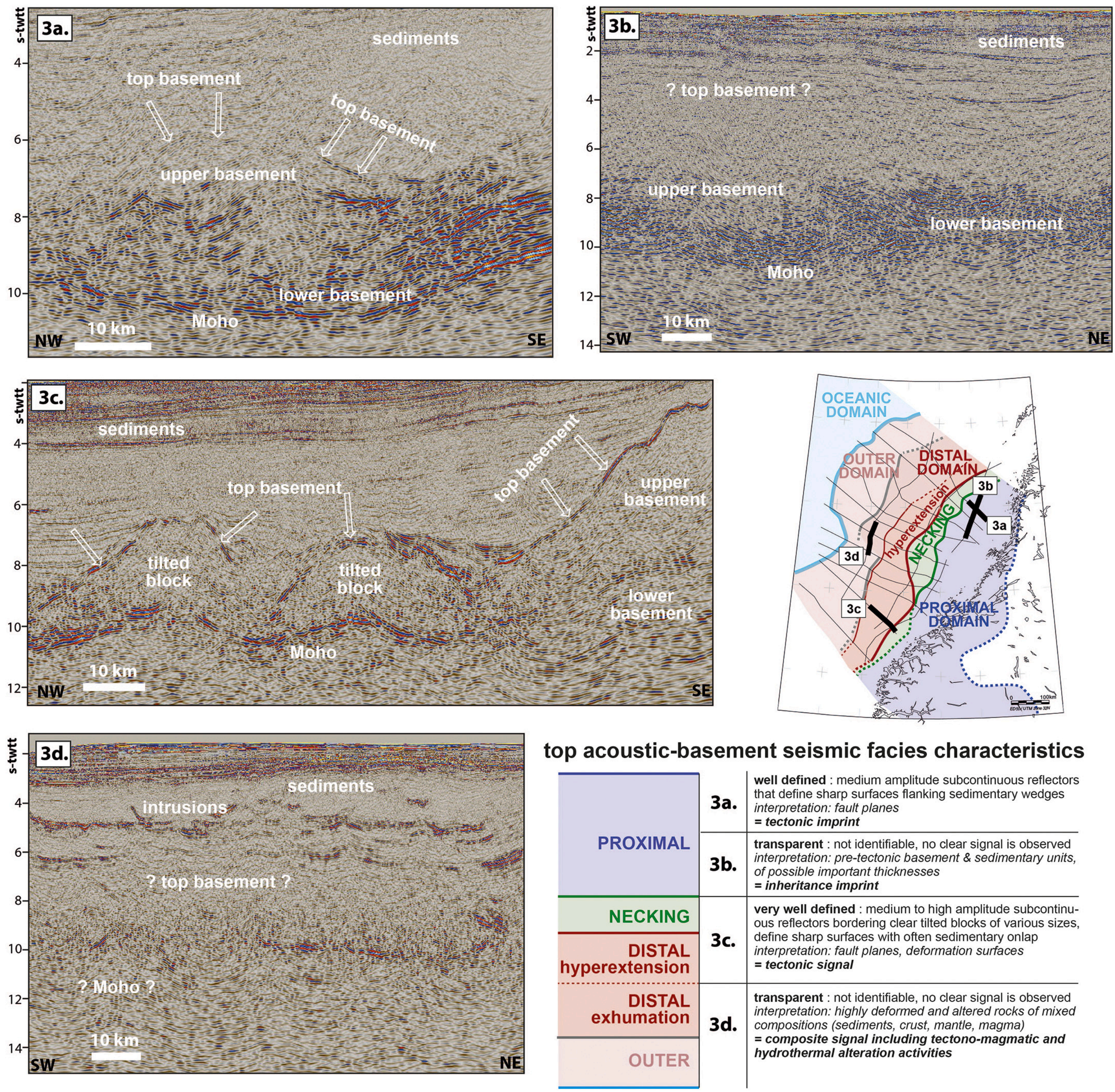

Fig. 3. Seismic extracts illustrating the different seismic facies observed for the top acoustic basement. See Fig. 1 for location. 3a. Seismic extract from the proximal margin showing a well-defined top acoustic basement (arrows). 3b. Seismic extract from the proximal margin showing a transparent top acoustic basement. 3c. Seismic extract from the hyperextension margin domain showing a very well-defined top acoustic basement (arrows). 3d. Seismic extract from the distal margin showing a transparent top acoustic basement. The map on the right illustrates the definition of the margin structural domains (e.g., Peron-Pinvidic and Osmundsen, 2018) that is explained in the Discussion section and presented in detail in Fig. 10.

Faleide et al., 2010). In the following Discussion, we will see that, based on today's modern dataset and concepts, this map may be slightly updated.

3. The Geoex MCG RDI19 dataset

The Regional Deep Imaging 2019 (RDI19) data were acquired with Rosgeo's Akademik Lazarev in the late summer of 2019. RDI19 is a part of the larger Regional Deep Imaging (RDI) Project consisting of more than 16,000 km of long offset data in the Barents Sea, the Norwegian Sea and the North Sea (Norway, United Kingdom, Denmark and Faroe Islands). To image the very deep structures, such as the lower crust and Moho, Geoex MCG deployed a large source of 6270 in^3 and a 12,000 m long streamer. The first part of the streamer was towed slanted from 15 m to 30 m, while the last part was towed flat at a depth of 30 m. The data were recorded in continuous mode with a record length of 16 s-twtt (second two travel time). The data were processed by Down Under Geosolutions (DUG) using the newest deblending and deghosting techniques. The processing was designed to obtain the best imaging of the deep lithological units, including pre-migration noise attenuation, migration velocity model analysis, 2D Kirchoff pre-STM migration, prestack noise and diffracted multiple attenuation (Peron-Pinvidic and Åkermoen, 2020).

4. Observations, discussions and interpretations

To correctly analyse the geometry of a rifted margin, it is necessary to identify the core envelopes that delineate the main units constituting the geological system: the seafloor, the top basement and the Moho. The combination of these core envelopes provides very useful indicators of the global margin architecture and tectonic development (see for instance Reston, 2009; Franke, 2013; Peron-Pinvidic et al., 2013; Savva et al., 2014; Clerc et al., 2018). Their relative positions give direct information about the thicknesses of the defined units (sediment, basement) and hence deformation history of the margin, like the amount of crustal thinning and uplift-subsidence history.

Based on the Geoex MCG RDI19 dataset, we mapped the main sedimentary intervals, the main bordering faults, the top acoustic basement, the Moho, and analyzed their geometrical variations, structural details and seismic facies. Below, we summarize our observations and main findings regarding more specifically the top basement, the basement/crustal units, the Moho and the mantle. Short discussions are developed to introduce possible interpretations.

4.1. Top (acoustic) basement

4.1.1. Definition

The top basement is a difficult term to use as it can have various meanings, possibly generating misunderstanding. In an ideal text-book situation, the top of basement should correspond to the top of the crystalline continental crust that constitutes the basis on which the rift initiates. In that context, the top basement should be a sharp lithological interface in between continental crust and rift-related sediments. The density contrast would then generate a strong impedance contrast generating a reflector with large amplitudes on standard seismic reflection profiles. In reality, rifting rarely initiates on a clean homogeneous crystalline surface (Manatschal et al., 2014). The pre-rift setting is shaped by various previous tectonic events such as the orogeny and its collapse phase that affected the Norwegian region (e.g. for the North Sea case: Fazlikhani et al., 2017; Fossen et al., 2014; Lenhart et al., 2019; Phillips et al., 2016). Thus, pre-rift sedimentary records and deformed rocks of various lithologies, may be present when rifting initiates. So, in that context, the 'top of basement' term may be misleading. This relates directly to questions such as where, when and how rifting begins? Although fundamental, these questions are still unanswered in most rift settings (Peron-Pinvidic and Osmundsen, 2020; Peron-Pinvidic et al., 2020).

4.1.2. Observations

For the present study, to embrace the potential complex tectonic history of the region, we chose to map the 'top of basement' as the 'base *syn*-rift', i.e. the basis on which rifting initiates, whatever lithology it is. With a rift system presenting an extensional evolution over more than 300 Myrs, the limitation in that case is that the different margin domains have different phases of tectonic activity, which lead to the definition a composite envelope at the margin-scale, of variable composition, age and origin.

Concretely, our top of basement corresponds to the base of the well identified sediments / layered sequences with characteristic stratigraphic geometries (e.g. wedges, erosional surfaces, contacts) (Fig. 3). Distinction is made with the usually more transparent to more chaotic disorganized unit below. The mapped horizon presents variable seismic facies. For instance, in some places, the top acoustic basement is clearly identified by well-defined sharp reflectors bounding syn-tectonic sedimentary wedges: Fig. 3a shows an example from the proximal margin Trøndelag Platform where the top acoustic basement has been mapped as corresponding to a fault plane onlapped by sedimentary diverging layers. However, at other locations in this same proximal domain, the top acoustic basement is impossible to identify (see the example proposed in Fig. 3b). In the hyperextension domain, the base of the syn tectonic sedimentary sequences and fault planes are clearly imaged and the top acoustic basement is easily mapped along well-defined tilted blocks / half grabens (e.g. the hyperextension domain in Møre, Fig. 3c). Further oceanward, in the distal domain, the top acoustic basement is very difficult to identify. Fig. 3d shows an extract from a profile located in the deep Møre Basin where no specific geometry or reflector can be recognized at depth under the thick sedimentary successions.

4.1.3. Interpretation

Based on the above observations, it can be concluded that the top acoustic basement along the Norwegian Continental Shelf presents different seismic facies and geometries along the margin. The proximal settings can present opposite facies characteristics from unambiguously sharp (e.g., fault planes, Fig. 3a) to seismically invisible limits (Fig. 3b). Interestingly, the other regions present more regular characteristics with the systematic absence of identifying features in the distal domain, and a clear demarcation identified in the necking and hyperextension domains (Fig. 3 cd). Based on this, it can be concluded that the seismic facies of the top acoustic basement mostly match the margin structural domains definition (Peron-Pinvidic and Osmundsen, 2018) - with two possible options in the proximal domain (either well defined or transparent), very well defined surfaces in the necking and hyperextension domains and no signal in the exhumation and outer domains (see Fig. 3 bottom right summary Table). These structural domains were defined based on the tectonic development of the rifted margin (Peron-Pinvidic et al., 2013). So, the top acoustic basement appears to be mostly related to the tectonic imprint that the margin undergoes during rift evolution. The clearly identifiable sharp reflectors can be interpreted as fault planes and deformation-related surfaces. The absence of clear seismic horizons may be related to various factors. In the case of the distal settings, high levels of deformation are often assumed, which may lead to the formation of new surfaces (exhumed rocks) possibly extensively deformed and altered (e.g. rock remobilization, hydrothermal alteration in highly fractured units, serpentinization, melt intrusions). These reactions may lead to alteration and metamorphism over important thicknesses of rocks. Such lithological changes may prevent the genesis of any clear seismic reflection horizon (e.g., Griffin and O'Reilly, 1987b; Mooney, 1992). The presence of thick sedimentary intervals at great depths, enhancing compaction and densification processes can also prevent the genesis of a clear seismic signal. This hypothesis may be advocated for the proximal settings where deep basins developed over thinned crust (Peron-Pinvidic et al., 2020).

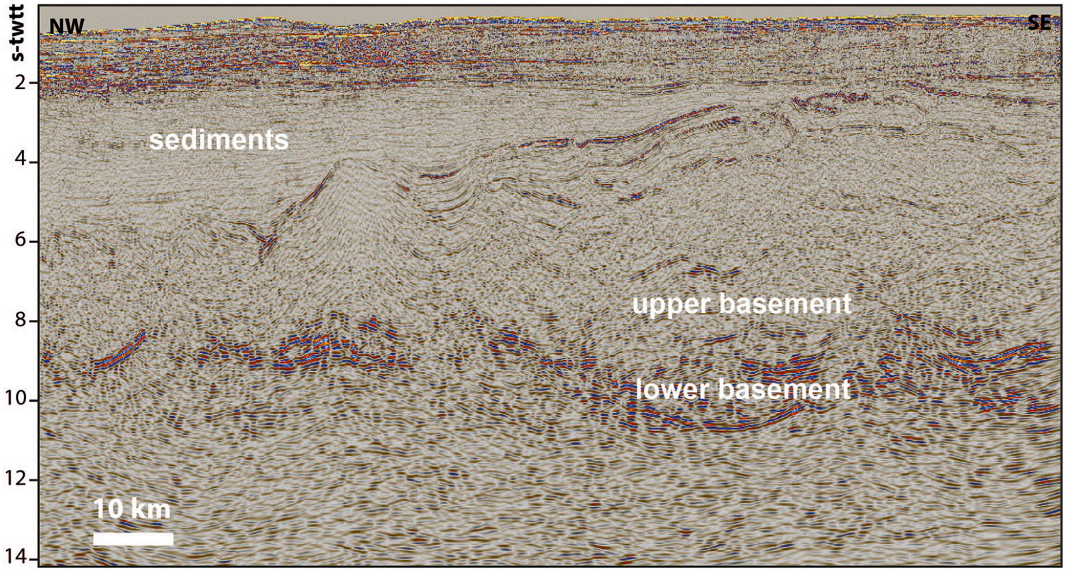

Fig. 4. Seismic extract illustrating the different seismic facies of the upper and lower parts of the basement. See Fig. 1 for location.

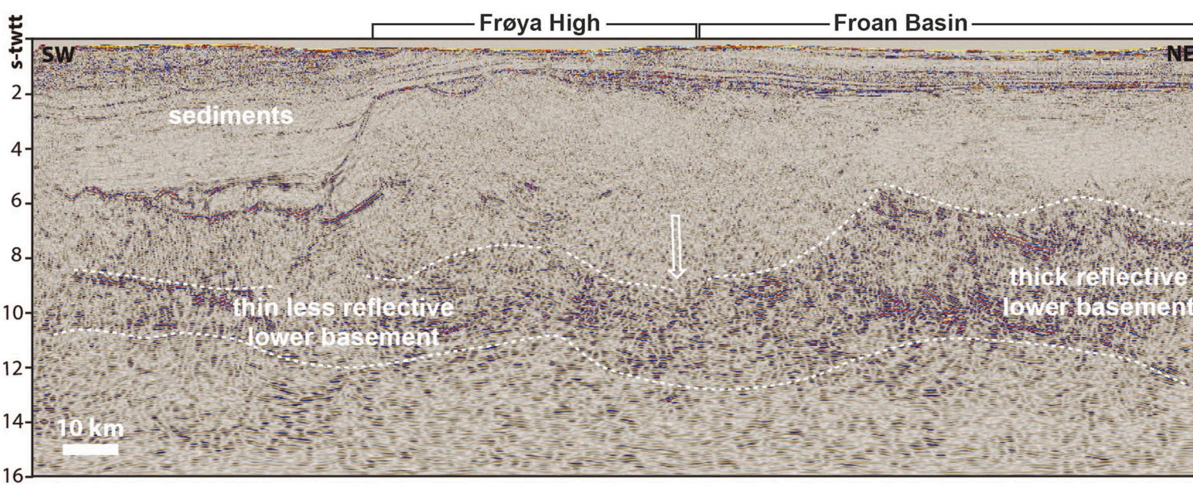

Fig. 5. Seismic extract illustrating the along-strike lateral variation of the upper vs. lower basement seismic facies partition. See Fig. 1 for location.

Thus, at margin-scale, the top acoustic basement appears as a composite surface that can carry both a *syn*-rift tectonic and an inheritance signal (Fig. 3). Depending on the local structural context, both can contribute to the seismic facies and geometrical characteristics.

4.2. Upper and lower basement units

4.2.1. Observations

The unit comprised in between the top-acoustic-basement and the Moho is here termed basement, without any preconceived interpretation of the corresponding lithology. This basement unit is characterized by a seismic facies partition distinguishing upper and lower basement units (Figs. 2, 4 and 5). However, the distinction is margin domain dependent with a clear distinction in the proximal and necking domains, sometimes including the hyperextension subdomain, but no distinction is observed in the more distal settings (see below).

The upper basement unit is very much transparent relative to the lower unit. The observed reflectors are mainly disorganized, chaotic and with low amplitude. On the contrary, the lower basement unit presents very distinct seismic facies, with high reflectivity and series of bright reflectors with medium to high amplitudes. There appears to be an oceanward density increase in the high amplitude reflectors with a change in organization pattern from mostly disorganized in the proximal domain to more subparallel and converging reflectors towards the necking domain with an overall strongly layered seismic facies (see for instance profile B on Fig. 2b).

This marked facies distinction between an upper and a lower basement unit is well defined in the Vøring segment. Southward, the distinction is less obvious in the Møre segment (Fig. 2a). Fig. 5 is an extract from an along-strike profile imaging the transition from the Møre to the Vøring segments. It shows the lateral variation from the northern clear seismic facies signature of the lower basement to the southern regions where it gets thinner and less reflective. The transition appears to correlate with the Frøya High area (Fig. 5) where the lower basement unit significantly thins, from ca. 6 to ca. 3 s-twtt thickness, with a radical change in seismic facies.

4.2.2. Interpretation

The lower basement's seismic facies may be due to various factors, including lithological, compositional, tectonic and magmatic hypotheses (e.g., Mooney, 1992). Some of the high amplitude reflectors may correspond to magmatic intrusions: mafic intrusions into lower crustal rocks can generate impedance contrasts strong enough to generate seismic amplitude changes; and multiple subparallel intrusion events could generate a layered pattern (Griffin and O'Reilly, 1987a; Carbonell et al., 2013). Although this hypothesis may be valid for some high reflectivity occurrences, the margin-scale observation may argue in favor of another option. Additionally, no systematic cross-cutting geometries, interpreted as characteristic of rift intrusions (Wrona et al., 2019), are observed. The pre-rift tectonic fabric could also be advocated: the pseudo-layered seismic facies may be related to pre-rift rock lithology and/or deformation phases, like orogenic nappe remnants or pre-rift orogenic collapse ductile deformation (Lenhart et al., 2019). Shear zones are notably recognized as deformation structures typical of the lower crust, and these can present important thicknesses and extend over huge areas (Clerc et al., 2015; Fazlikhani et al., 2017). Based on this tectonic hypothesis, the lower basement seismic facies changes could represent variations in deformation intensity: the lower basement can be interpreted as a layer that preferentially accommodated extensional deformation from relatively more distributed and diffuse in the proximal domain to more focused in the necking and hyperextension domains, with the lower basement thickness decrease oceanward representing the excision of the layer.

Along the same line of thought, along-strike, the important geometrical and facies changes observed at the level of the Frøya High may be related to the existence of specific ductile layers used to differentially accommodate collapse and rifting (Gresseth et al., 2021; Muñoz-Barrera et al., 2020).

4.3. Moho and upper mantle

4.3.1. Observations

The Moho is here mapped as the base of the lower basement high reflectivity facies (see Figures 2abc). Similar to the top basement described above, the facies and geometries vary substantially in the dip direction, from a diffuse pattern in the proximal setting to a more well-defined band of focused high amplitude reflectors in the hyperextension domain. The distal margin does not present any clear mappable Moho: the Vøring and Møre distal basins display thick sedimentary sequences, an acoustic top basement difficult to identify and a transparent Moho. No specific reflector or significant change in the seismic facies is observed that could be interpreted in terms of a Moho. More oceanward, in the Vøring segment, a series of high amplitude undulating reflectors appear in the outer domain that can be interpreted as Moho (Figures 2bc).

Interestingly, the imaging of the entire basement allowed by the Geoex MCG RDI19 dataset confirms the presence of some reflectors that used to be debated in the past - like, for instance, the 'DRB' (Deep Reflector Band) previously mapped and discussed by various authors (e.g., Osmundsen and Ebbing, 2008; Osmundsen et al., 2002). These reflectors are observed at crustal depths, usually between 8 and 10 s-twtt and were occasionally argued to correspond to seismic processing noise. The Geoex MCG RDI19 dataset shows that the DRB actually corresponds to some of the reflectors with high reflectivity at the base of the lower basement unit and consequently they probably correspond to real features.

Regarding the upper mantle, the signals are difficult to interpret. Given the depths at which the mantle is observed (usually >10 s-twtt), a legitimate question arises regarding the pertinence of analysing such geometries as these are often treated as artificial processing-related signal. However, the acquisition parameters and processing characteristics of the dataset (section 3) attest to good quality signal with reasonable imaging down to great depths. This argues in favor of extending the interpretation below 10 s-twtt. An additional argument for interpreting the mantle reflectivity is that the seismic facies characteristics observed below the Moho are systematically observed on all the profiles, with variations, which suggests real features. The profiles presented in the Figures 2abc show the facies zonation that can be observed at mantle depths (with the stippled white lines) distinguishing the proximal, distal and outer/oceanic domains. In the proximal, necking and hyperextension domains, a horizon can be mapped, usually ca. 2 s-twtt below the Moho, that separates an upper body of low amplitude disorganized small reflectors, with an overall chaotic seismic facies, from a lower body that appears more transparent, with low reflectivity and without any distinct events. In the distalmost and outer domains, there is a clear body with high amplitude disorganized multiple short reflectors that can be delineated at depth by a capping undulating envelope (see Figures 2ab). In between, in the distal-exhumation subdomain, there is no clear signal distinction, with no significant change in seismic facies.

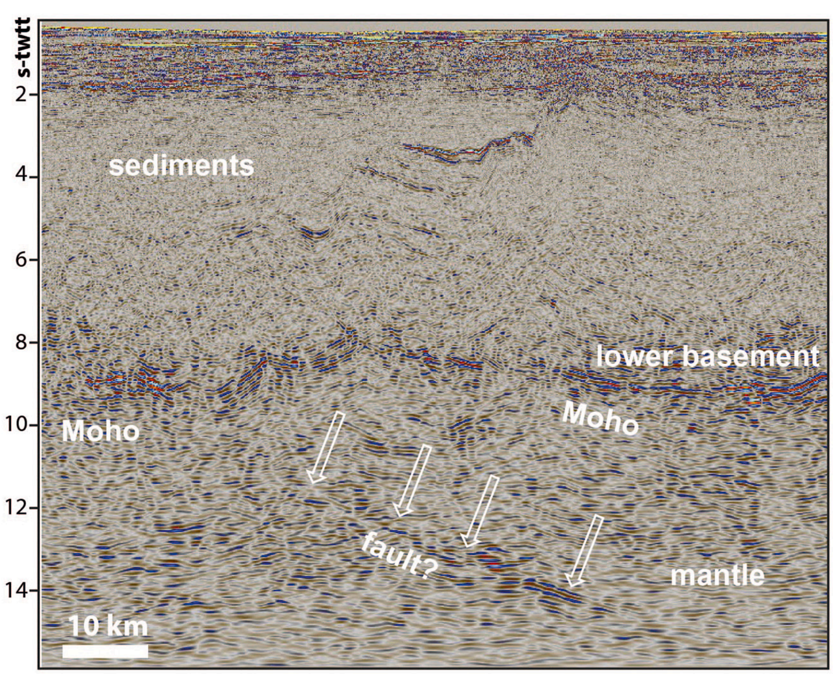

Fig. 6. Seismic extract illustrating the possible imaging of a fault in the upper mantle. See Fig. 1 for location.

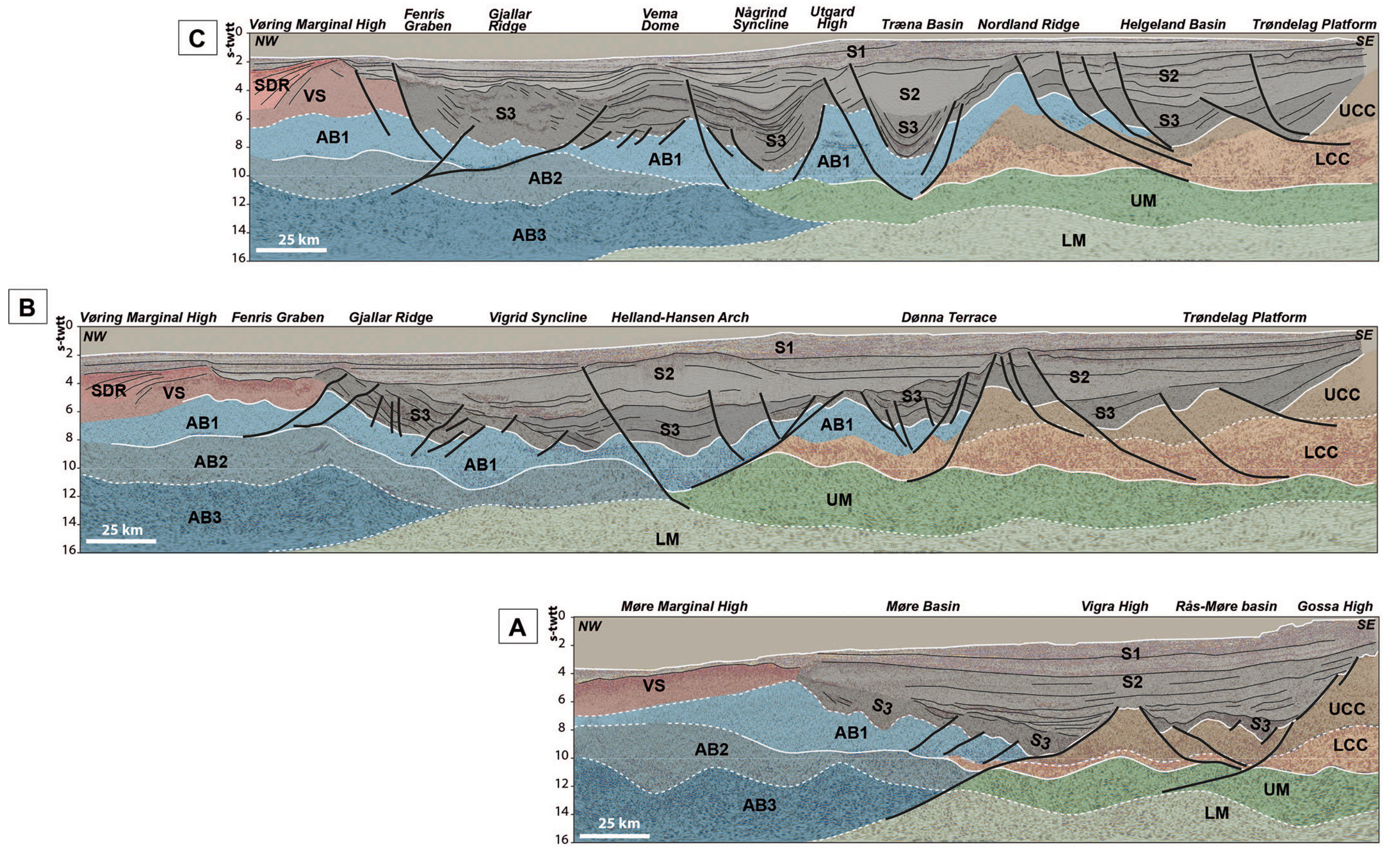

Fig. 7. The three selected key seismic reflection profiles (Fig. 2) with the outline of the main bodies that can be delineated based on basic seismic reflection observations. UCC upper continental crust. LCC lower continental crust. AB acoustic basement. UM upper mantle. LM lower mantle. VS volcanics-sediments. SDRs seaward dipping reflectors. S sediments. The main uncertainties relate to the composition of the AB bodies outlined in blue colours in the distal margin. The defined bodies serve as direct input for gravity modelling (Fig. 8). (For interpretation of the references to colour in this figure legend, the reader is referred to the web version of this article.)

4.3.2. *Interpretations*

As with the basement units, the seismic facies variations observed at mantle depths can be related to various factors as e.g., lithological, compositional and/or geochemical changes (Carbonell et al., 2013). In the absence of drilling constraints, interpretation of such deep rocks remains difficult.

Various research projects investigated the seismic reflection characteristics of the deep crust in extensional settings, such as the marine surveys BIRPS and MONA LISA (Klemperer and Hobbs, 1991; Snyder and Hobbs, 1999; Singh et al., 1998; MONA-LISA-working-group, 1997) that provided spectacular images of the Moho and upper mantle in the central North Sea. In the same area, various studies reported the possible presence of faults below the Moho (Bartholomew et al., 1993; Gabrielsen et al., 2015; Fossen et al., 2014). Interestingly, the Geoex MCG RDI19 dataset adds some observations to this catalogue with, locally, some well-defined sub-continuous reflectors with medium to high amplitudes observed below the Moho horizon. Fig. 6 shows an example of a signal observed at mantle depths, under the Dønna Terrace in the Vøring segment (see location on Fig. 1). Similar to the above cited North Sea observations, this reflector may be interpreted as a fault system, accommodating deformation at great depths below the crust. However, the signal is tenuous and alternative explanations may be valid, such as melt intrusions trapped in the upper mantle (Wrona et al., 2019).

5. Gravity models

Based on the above summarized observations, it appears that the Geoex MCG RDI19 dataset allows unprecedented observations to be made regarding the geometries, structures and seismic facies of key sedimentary and basement units. However, fundamental questions remain on the corresponding lithologies. In the absence of any well sampling, the lithology of the acoustic basement is mostly unconstrained, especially in the distal margin.

5.1. *Protocol*

Standard interpretation protocols often involve geophysical modelling at a second stage to help finalize the interpretations. The limitations in the approach being that any modelling is non-unique, resulting in the fact that various models can fit the observed data, although often only one is presented. To acknowledge these limitations, and investigate the range of possible interpretations, we proceeded to basic gravity modelling based on three scenarios. These have been selected to represent the range of possible interpretations that can be proposed for such rifted margin settings, including the two end-members 'crust' vs. 'exhumed mantle' approaches (see explanation below). In this study, on purpose, to keep the modelling exercise the most robust and to test the end-member scenarios in the most objective way: 1. The geometries of the modelled bodies strictly correspond to the observations mapped on the seismic reflection profiles; 2. The experiment is kept simple and basic with the fewest possible bodies; 3. No modifications of the mapped geometries are done at modelling stage; 4. Only the density values are varied and no attempt is made to fit the modelled anomaly to the observed anomaly curves.

Practically, the gravity modelling has been performed with the GM-SYS add-on tool under the GEOSFT software that allows $2^3/_4$ D

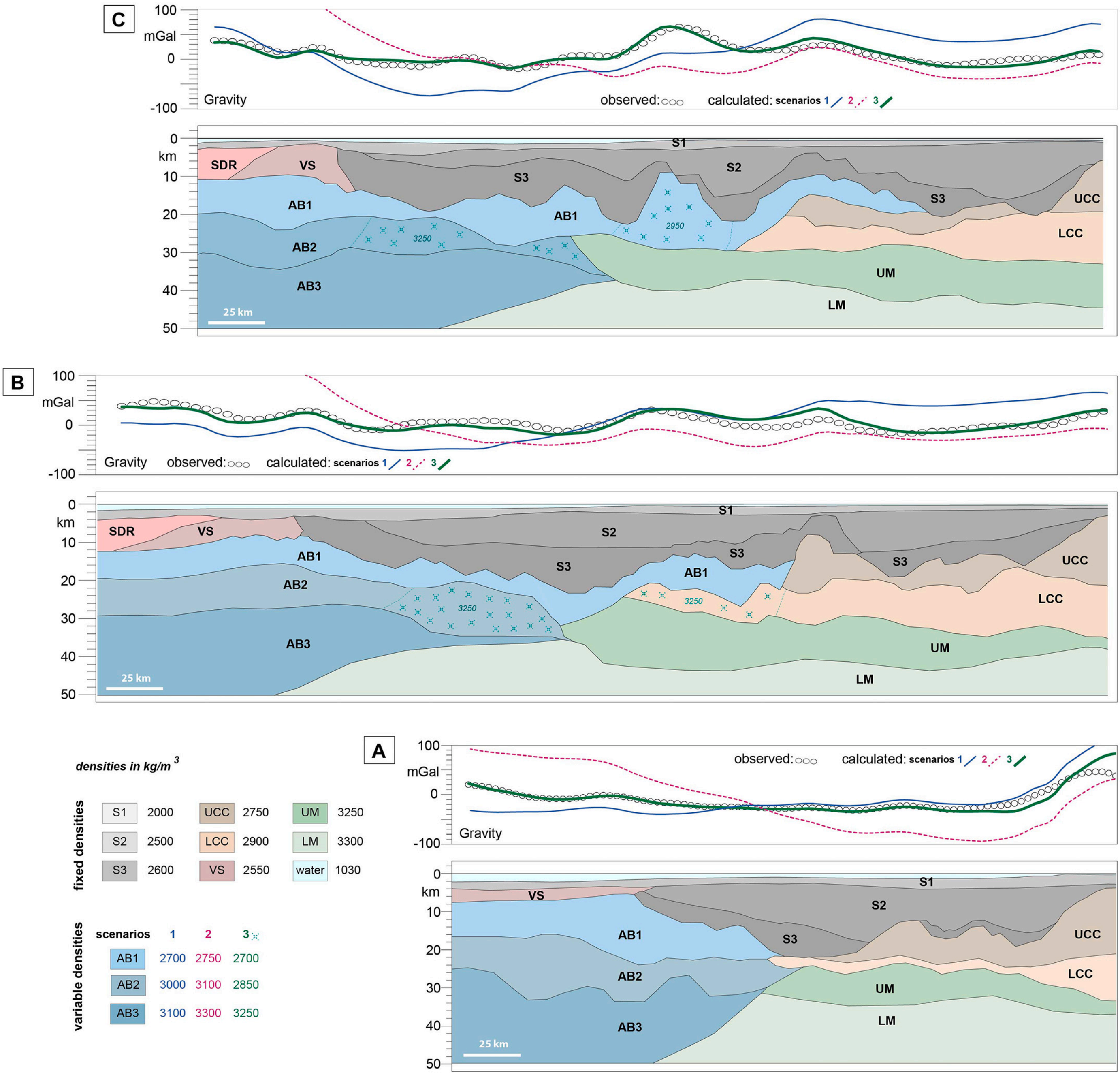

Fig. 8. Gravity modelling of the three selected profiles (Figs. 2 and 7). In order not to bias the modelling protocol and results, the bodies are defined based on observations from the seismic reflection profiles and are used directly in the modelling experiment without any geometrical modification. Only the density values are varied. The density values used for the sediments, continental crust and mantle bodies are standard values considered as representative of such units in the region (e.g. see data compilation by Peron-Pinvidic et al., 2012). The density values vary only for the AB bodies (blue colours in the distal margin). Three scenarios are tested according to the end-member scenarios proposed for such distal settings. See text for detailed description. (For interpretation of the references to colour in this figure legend, the reader is referred to the web version of this article.)

modelling. The bodies defined in the model are laterally extended by 50 km to avoid edge effects. The models stop at 80 km depth in order to well capture the effects of all the bodies at depth. The observed gravity curve used for the modelling has been extracted from the Free Air Gravity map produced for the NAG-TEC project (Hopper et al., 2014).

5.2. Input

Fig. 7 shows the three key profiles with the outlines of the main units used in the modelling procedure. Sedimentary units are interpreted down to the top acoustic basement envelope. A distinction is made between the shallow Cenozoic interval (S1) from the deeper sequences S2 and S3 of potentially higher density values. For instance, S3 is individualized to represent the deepest sedimentary units that are potentially more compacted at the base of the basins, and the outer sequences that can be altered / intruded by magmatic material in the outer margin. The presence of volcanics and seaward dipping reflectors (SDR) in the outer margin is modelled with the bodies labelled 'VS' (volcanics-sediments) and 'SDR' (see Fig. 7). The basement is interpreted in terms of upper continental crust (UCC) and lower continental crust (LCC) bodies in between the top acoustic basement and Moho envelopes in the proximal parts of the sections (see brownish colours on Fig. 7). Below, the mantle is divided into two units, an upper (UM) and a lower mantle (LM) based on the seismic facies change described in the above section. All these units are attributed constant densities with values selected as the most representative of the assumed corresponding lithologies for sediments and continental crust. See for instance the compilation proposed by Peron-Pinvidic et al. (2012) for the region (based on Reynisson et al., 2010; Mjelde et al., 1998; Raum et al., 2002; Fernandez et al., 2004; Osmundsen and Ebbing, 2008).

The only variables in the modelling approach are the density values attributed to the bodies coloured in blue in Figs. 7 and 8. These are labelled 'AB' for acoustic basement. AB1 corresponds to the uppermost part of the acoustic basement. It is a relatively unstructured and transparent unit, often difficult to delineate with accuracy. The AB2 body corresponds to the basement distinguished below the Moho in the distal and outer margin domains, whereas the AB3 body is outlined below, based on the mantle high reflectivity facies mapped in the outer margin (Fig. 7).

5.3. Scenarios

As briefly introduced above, discussions about the composition of the corresponding rocks are still ongoing and interpretations are potentially very different. Unfortunately, no core constraint exists, and uncertainties will most certainly remain for a long time since no well can presently attempt to sample rocks at such great depths. Depending on the margin domain and structural setting, lithologies can span a wide range of options from sediments, volcanics, upper continental crust, lower continental crust, intrusions, mantle, mafic underplating, etc. Given its structural position, the AB1 body can correspond to various lithologies including for instance compacted sediments and/or deformed continental crust and mantle. Similarly, the composition of the AB2 body is unconstrained. It is typically outlined in between ~8 and 11 s-twtt - depths that should correspond to mantle rocks in these deep margin settings. However, the Mid Norwegian margin is recognized as a margin affected by a heavy magmatic imprint at the oceanization stage, so deformation, fluid circulation, hydrothermal alteration and magmatic intrusion / underplating are highly probable. Consequently, the composition of the AB2 and AB3 bodies could also span a wide range of lithological ultramafic and magmatic options.

In order to test the various hypotheses, two end-member scenarios have been delineated (scenario 1 - blue thin curve and scenario 2 - dashed purple curve on Fig. 8):

1. Scenario 1 assumes that the continental crust is excised in the hyperextension sub-domain and that the distal margin is floored by exhumed altered mantle and covered by sediments. Along that line of thoughts, the AB1 body (2700 kg/m^3) would correspond to a mix of sediments (compacted, altered, deformed and/or intruded) lying above an exhumed altered mantle (serpentinized, deformed). The AB2 and AB3 bodies would then correspond to different parts of a deformed mantle with attenuated densities of 3000 and 3100 kg/m^3.
2. At the other end of the spectrum of possible interpretations, scenario 2 assumes that the distal margin is floored by continental crust and magmatic underplated material. In that context AB1 would correspond to continental crust (density of 2750 kg/m^3), AB2 to underplated magmatic material (the so-called LCB - lower crustal body, or HVLC - high velocity lower crust; density 3100 kg/m^3), and AB3 to mantle (density 3300 kg/m^3).
3. A third scenario is then defined as an intermediate possibility. This scenario 3 was built selecting the densities providing the best gravity

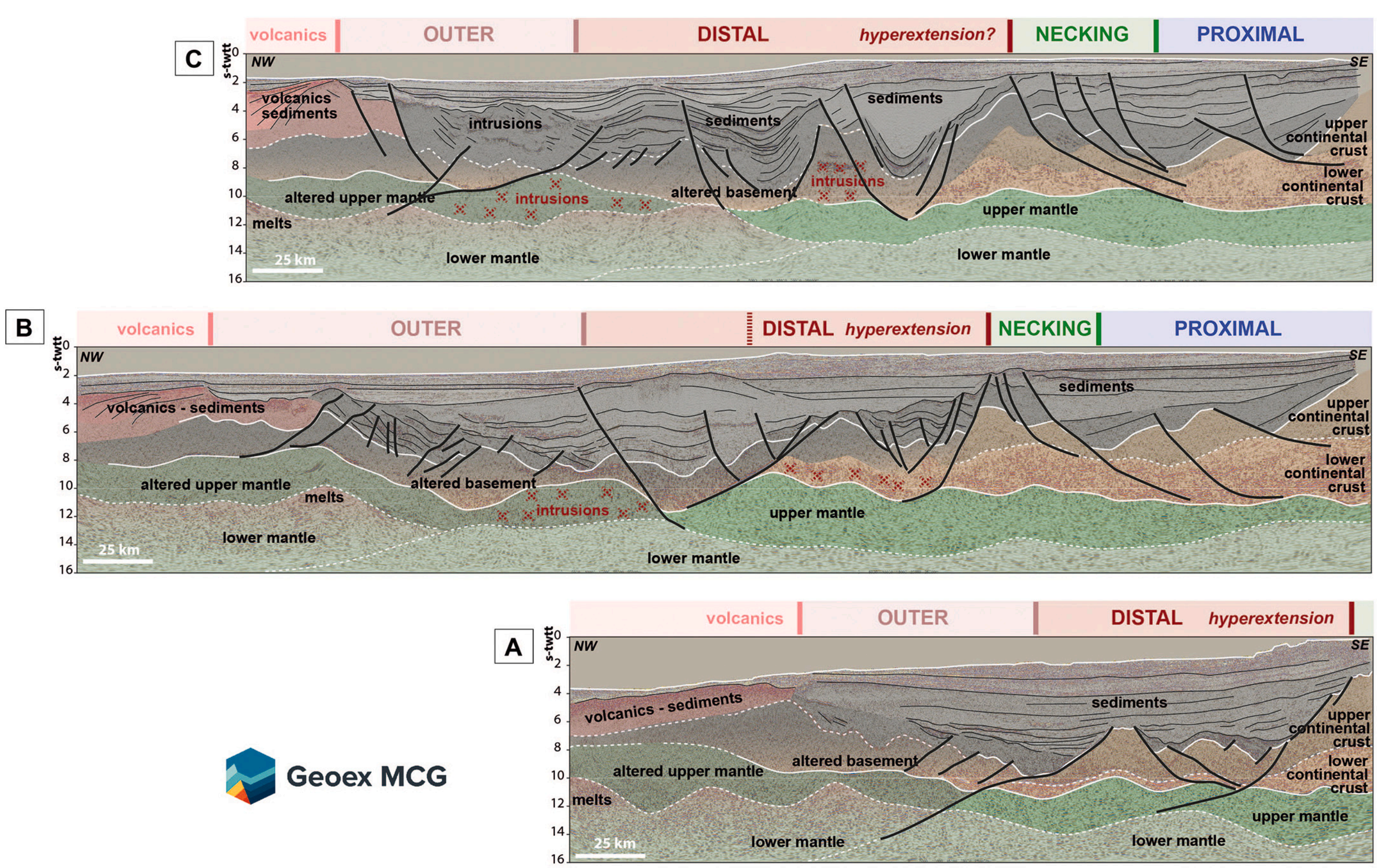

Fig. 9. Proposed interpretation of the selected profiles ABC. See text for further explanation. The altered basement unit is supposed to encompass combinations of sediments, continental crust and mantle, possibly heavily altered.

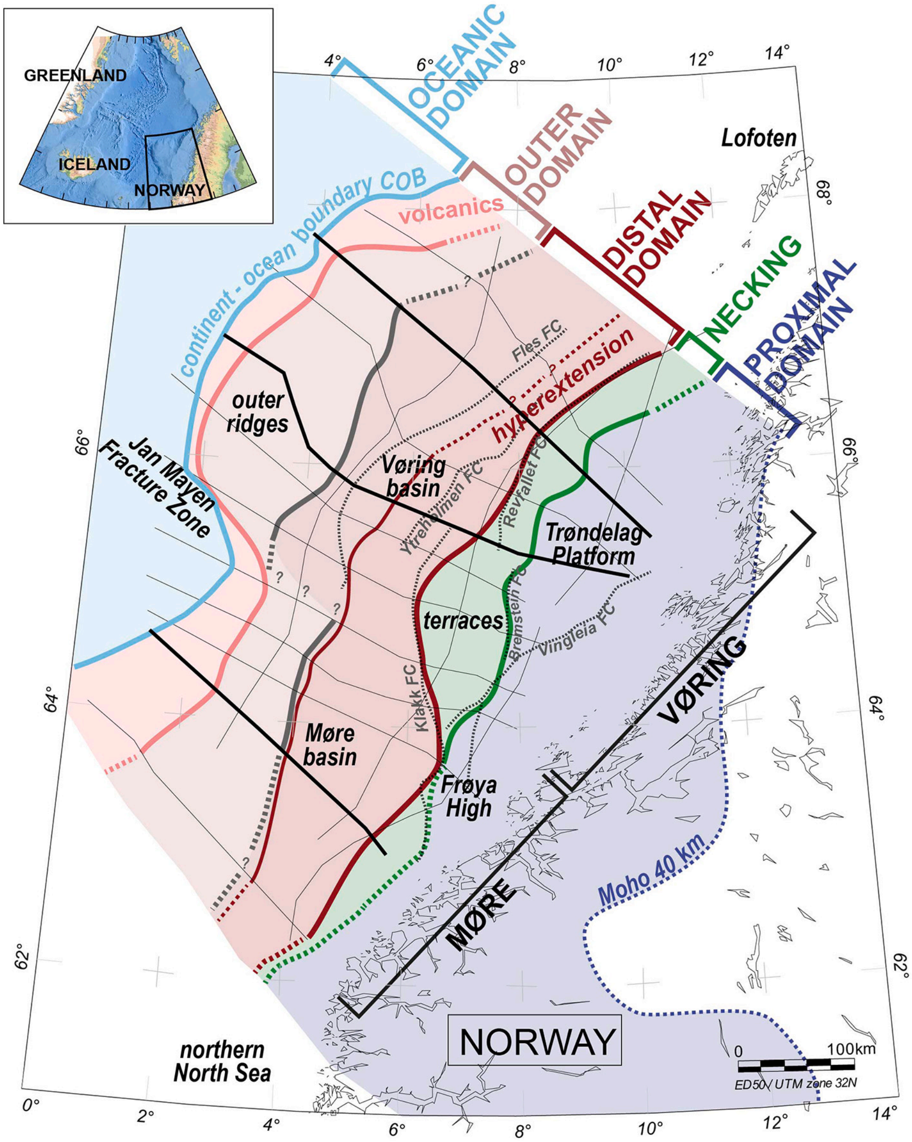

Fig. 10. Updated map of the Norwegian Continental Shelf with the outline of the margin domains: proximal (dark blue), necking (green), distal (red), outer (light pink) and oceanic (light blue). The ABC black lines locate the key profiles and the thin grey dashed lines locate the main fault complexes (FC) usually presented as main bordering structures (Fles, Ytreholmen, Klakk, Bremstein, Vingleia). (For interpretation of the references to colour in this figure legend, the reader is referred to the web version of this article.)

curve matches with no a priori assumptions on the lithologies. This scenario allowed for two further basic modifications to the modelled bodies to best fit the anomalies in the middle part of the B and C profiles with the addition of higher density bodies on both sides of the Fles Fault Complex (see green crosses on Fig. 8).

5.4. Interpretations

Fig. 8 highlights the good results provided by scenario 3 (green thick curve) - the scenarios 1 and 2 being less satisfying. Obviously, as for every modelling experiment, alternative geometries, other density values and 3D modelling approaches would give different results. As described above, models are non-unique. The experiment proposed here simply shows that intermediate alternatives with simple geometrical input and standard density values can explain the observed gravity signals, with no need for including multiple complicated bodies with particular physical parameters. The structural observations mapped on seismic reflection profiles associated with average density values are robust enough to generate models that satisfy the gravity observations.

Regarding the interpretation, the values attributed to the AB bodies in scenario 3 are compatible with intermediate scenarios of interpretation and with numerical modelling experiments that prove the possible presence in these distal settings of exhumed accreted new basement/crust (e.g. Lavier and Manatschal, 2006; Brune et al., 2014; Naliboff et al., 2017; Fourel et al., 2019). As illustrated on Fig. 9 with the label 'altered basement', the AB1 body could correspond to a mixture of remobilized sediments and altered exhumed basement (continental crust and/or mantle), including the probable presence of crustal allochthons issued from the various rifting deformation phases. The hypothesis was early suggested for e.g. the outer Vøring region (Lundin and Doré, 1997; Ren et al., 2003; Peron-Pinvidic and Osmundsen, 2016) and recently confirmed by drilling results (IODP Expedition 396). Below, the AB2 body could correspond to an upper mantle unit possibly affected by some magmatic intrusions. Meanwhile, the AB3 body could correspond to lower mantle rocks with high densities and potentially some melt accumulations at some locations (e.g. the corrugated surface delimiting AB2 and AB3 identified on the seismic reflection profiles). This scenario also emphasizes the structural role of the Fles Fault Complex in the architecture of the Norwegian Continental Shelf. In addition to being a major large scale and noticeable out-of-sequence structure, our basic gravity modelling suggests that it is associated with specific local higher density values (crosses on Figs. 8 and 9). These can be interpreted in terms of local magmatic intrusions, with the Fles Fault Complex playing a favoured role in the transport and emplacement of the related melts.

6. Map of the margin structural domains

As illustrated with this contribution, the Geoex MCG RDI19 dataset allows the first comprehensive mapping of the entire Mid Norwegian rifted margin. The above-described analysis protocol allows the building of a detailed interpretation of the seismic reflection profiles, with the identification and mapping of the rifted margin domains, main sedimentary basins and bordering tectonic structures (Fig. 9). The same interpretation procedure has been used for the whole dataset permitting the construction of a map of the margin structural domains, that is proposed in Fig. 10. The dark blue, green, red, pink and light blue polygons correspond, respectively, to the proximal, necking, distal, outer and oceanic domains, as defined initially by Peron-Pinvidic et al. (2013).

- The inner limit of the proximal domain is mapped as the geophysically modelled 40 km crustal thickness line, mostly located onshore (Osmundsen and Redfield, 2011; Funck et al., 2016a; Funck et al., 2016b; Funck and NAG-TEC-Group, 2014).
- The proximal domain is characterized by the strong crustal division between the upper relatively transparent unit and the lower highly reflective unit. This domain of the margin is understood to be very much dependent on the pre-rift inheritance (Manatschal et al., 2014). The basement is interpreted as mostly crystalline crust, including remnants of orogenic nappes and orogenic collapse structures and related sedimentary basins. From outboard of the 40 km thickness line, the basement is substantially thinned down to 20–30 km. High levels of structural complexity with combinations of shear zones, detachment faults, core complexes and ultra-thinned crust are observed at some locations (e.g., Helgeland Basin; Peron-Pinvidic et al., 2020), which attest to the potential high intensity of local deformation.
- The landward limit of the necking domain (green line on the Fig. 10 map) is identified where the Moho begins to steadily rise, with a significant change in the seismic facies of the lower basement unit towards focused and converging bands of reflectors. The necking domain corresponds to the area of the margin where the top acoustic-basement and Moho core envelopes converge attesting to significant basement thinning and probable excision of the mid-lower crustal ductily deformed rocks.
- The landward limit of the distal domain (thick red line on the Fig. 10 map) is mapped from where the sedimentary accommodation space increases drastically. This increase archives the evidence for an important basement thinning that led to significant subsidence, allowing for sedimentary accumulation. Structurally, the hyperextension domain corresponds to series of rotated blocks, with very well-defined geometries of half-grabens and tilted blocks, flanked by clearly identifiable faults.
- The thin red line within the distal domain on Fig. 10 is mapped at the oceanward limit of the series of tilted blocks of the hyperextension domain. The most oceanward part of the distal domain is difficult to analyse as few seismic signals are observed. No top acoustic basement or Moho are identified. The base of the sedimentary sequence is very chaotic to very much transparent and no geometry can be robustly delineated. The architecture of this part of the margin remains thus unconstrained.
- The landward limit of the outer domain (grey line on the map) is mapped where an uplift and/or back rotation of some stratigraphic layers are observed. This configuration is interpreted as witnessing the presence at depth of some structural ridges accommodating specific uplift-subsidence patterns, which are considered as representative of the outer domain (e.g., Ren et al., 2003; Lundin and Doré, 1997).
- A pink line is displayed on the Fig. 10 map within the outer domain to mark the location of the lava flows escarpment, a specific geometry related to the volcano-magmatic evolution of the outer margin towards the oceanic domain (Geissler et al., 2016).
- The continent-ocean boundary (COB) is represented with a light blue line on the Fig. 10 map. It corresponds to the boundary proposed by Gaina et al. as marking the definitive end of the continental environment (the rifted margin) and the beginning of the oceanic crust *s. s.* (Gaina, 2014; Gaina et al., 2017).

The resulting map illustrates the composite nature of the Norwegian Continental Shelf with well-defined structural domains. Additionally, the map confirms the strong structural partition existing between the Møre and Vøring segments. This highlights the importance of the structural axis delineated by the margin segments and the Jan Mayen Fracture Zone in the oceanic domain. In the direct inboard projection of that major tectonic lineament, the Frøya High appears as a pivot structure, of probably key significance for the local geodynamic evolution. Detailed study and mapping are needed there to correctly constrain this region of probable major tectonic importance (e.g. Gresseth et al., 2021).

This map of the structural domains also shows an interesting match between the margin domain limits and the fault complexes (FC) dissecting the margin basement and delimiting the sedimentary basins (medium size stippled dark grey lines on the Fig. 10 map) (Blystad et al., 1995). For instance, the Klakk FC corresponds to the inner distal boundary, and the Bremstein FC to the inner necking boundary. However, some fault system appears more isolated such as the Fles FC which lies out-of-sequence within the distal domain of the Vøring segment.

7. Conclusions

This contribution summarizes a study of the RDI19 dataset provided by Geoex MCG. The dataset consists of 15 regional deep penetrating long-offset seismic reflection profiles allowing an unprecedented imaging of the entire Mid-Norwegian rifted margin, including deep basement/crustal units, Moho, and upper mantle.

Our main findings can be summarized as follows:

1. The dataset allows - for the first time - the identification, analysis and mapping of the entire margin architecture from seafloor to the upper mantle, including the lower basement/crustal units and Moho, from the most proximal settings to the continent ocean boundary.
2. The top acoustic basement is well identified where the tectonic imprint is dominant vs. the inheritance signal, like in the necking and hyperextension domains where it is commonly associated with well imaged fault planes. Elsewhere it is regularly difficult to observe as there is a high level of deformation and alteration processes that may affect the related seismic signal, like in the distal margin domain.
3. In the proximal and necking margin domains, the acoustic basement is clearly divided into an upper transparent unit and a lower highly reflective unit.
4. The Moho presents seismic facies and geometrical variations directly matching the margin tectonic domains, from a globally diffuse pattern in the proximal margin, convergent in the necking domain and very much focused in the hyperextension domain, to a transparent facies in the distalmost settings and undulating in the outer domain.
5. Uncertainties remain regarding the composition of the distal and outer margin acoustic basement rocks. Basic gravity modelling was used to test end-member interpretations (crust vs. mantle vs. combinations interpretation scenarios). The modelling does not require complex geometries or particular inputs to fit the observed gravity curves. Standard density values and simple structural mapping lead to very good model results.

6. Based on the observations and modelling exercises, an updated map of the margin structural domains is proposed (Fig. 10).
7. Our results confirm the core structural role of the Jan Mayen Fracture corridor and of Frøya High as pivot structures in the global architecture of the Norwegian Continental Shelf.

Credit author statement

Gwenn Peron-Pinvidic: Formal analysis, Investigation, Project administration, Conceptualization, Methodology, Writing, Reviewing, Editing, Visualization. Tor Åkermoen: Project administration, Reviewing, Editing. Lars Ivar Leivestad: Project administration, Reviewing, Editing.

Declaration of Competing Interest

The authors declare that they have no known competing financial interests or personal relationships that could have appeared to influence the work reported in this paper.

Ackowledgements

Geoex MCG is acknowledged for data access and display authorization, and Schlumberger for providing the Petrel seismic interpretation software. Kim Welford and Alvar Braathen are acknowledged for their pertinent and very useful suggestions and corrections.

References

Bartholomew, I.D., Peters, J.M., Powell, C.M., 1993. Regional structural evolution of the North Sea: Oblique slip and the reactivation of basement lineaments. In: Parker, J.R. (Ed.), Petroleum Geology of Northwest Europe: Proceedings of the 4th Conference. Geological Society, London, pp. 1109–1122.

Blystad, P., Brekke, H., Færseth, R.B., Larsen, B.T., Skogseid, J., Tørudbakken, B., 1995. Structural elements of the Norwegian continental shelf, Part II. The Norwegian Sea Region. Norw. Petrol. Direct. Bull. 8, 0–45.

Brekke, H., 2000. The tectonic evolution of the Norwegian Sea Continental margin with emphasis on the Vøring and Møre Basins. In: Nøttvedt, A. (Ed.), Dynamics of the Norwegian Margin: Geological Society Special Publication. Geological Society of London, UK, pp. 327–378.

Brune, S., Heine, C., Pérez-Gussinyé, M., Sobolev, S.V., 2014. Rift migration explains continental margin asymmetry and crustal hyper-extension. Nat. Commun. 5.

Carbonell, R., Levander, A., Kind, R., 2013. The Mohorovičić discontinuity beneath the continental crust: an overview of seismic constraints. Tectonophysics 609, 353–376.

Clerc, C., Jolivet, L., Ringenbach, J.-C., 2015. Ductile extensional shear zones in the lower crust of a passive margin. Earth Planet. Sci. Lett. 431, 1–7.

Clerc, C., Ringenbach, J.-C., Jolivet, L., Ballard, J.-F., 2018. Rifted margins: Ductile deformation, boudinage, continentward-dipping normal faults and the role of the weak lower crust. Gondwana Res. 53, 20–40.

Færseth, R.B., 2020. Structural geology and basin development of the Norwegian Sea. Nor. J. Geol. 100.

Faleide, J.I., Tsikalas, F., Breivik, A.J., Mjelde, R., Ritzmann, O., Engen, Ø., Wilson, J., Eldholm, O., 2008. Structure and evolution of the continental margin off Norway and the Barents Sea. Episodes 31, 82–01.

Faleide, J.I., Bjørlykke, K., Gabrielsen, R.H., 2010. Geology of the Norwegian continental shelf. In: Bjørlykke, K. (Ed.), Petroleum Geoscience: From Sedimentary Environments to Rock Physics, pp. 467–499.

Fazlikhani, H., Fossen, H., Gawthorpe, R.L., Faleide, J.I., Bell, R.E., 2017. Basement structure and its influence on the structural configuration of the northern North Sea rift. Tectonics 36, 1151–1177.

Fernandez, M., Torne, M., Garcia, C.D., Verges, J., Wheeler, W., Karpuz, R., 2004. Deep structure of the Voring margin; the transition from a continental shield to a young oceanic lithosphere. Earth Planet. Sci. Lett. 221, 131–144.

Fossen, H., 2000. Extensional tectonics in the Caledonides: Synorogenic or postorogenic? Tectonics 19, 213–224.

Fossen, H., 2010. Extensional tectonics in the North Atlantic Caledonides: a regional view. In: Law, R., Butler, R., Holdsworth, B., Krabbendam, R.A., Strachan, M. (Eds.), Continental Tectonics and Mountain Building: The Legacy of Peach and Horn. Geological Society Special Publication, London, pp. 767–793.

Fossen, H., Gabrielsen, R.H., Faleide, J.I., Hurich, C.A., 2014. Crustal stretching in the Scandinavian Caledonides as revealed by deep seismic data. Geology 42, 791–794.

Fourel, L., Buiter, S., Peron-Pinvidic, G., 2019. Reappraisal of the Norwegian Proximal Domain: from Devonian Orogenic Collapse to Mesozoic rift Extension - Numerical Modelling (NGU), G.S.o.N. (Ed.), Trondheim, p. 132.

Franke, D., 2013. Rifting, lithosphere breakup and volcanism: Comparison of magma-poor and volcanic rifted margins. Mar. Pet. Geol. 43, 63–87.

Funck, T., NAG-TEC-Group, 2014. Crustal structure, Chapter 6. In: Hopper, J.R., Funck, T., Stoker, M., Árting, U., Peron-Pinvidic, G., Doornenbal, J.C., Gaina, C. (Eds.), Tectonostratigraphic Atlas of the North-East Atlantic Region. GEUS, Copenhagen.

Funck, T., Erlendsson, Ö., Geissler, W.H., Gradmann, S., Kimbell, G.S., McDermott, K., Petersen, U.K., 2016a. A review of the NE Atlantic conjugate margins based on seismic refraction data. In: Peron-Pinvidic, G., Hopper, J.R., Stoker, M., Gaina, C., Funck, T., Arting, U., Doornenbal, J.C. (Eds.), Geological Society. Special Publications, London.

Funck, T., Geissler, W.H., Kimbell, G.S., Gradmann, S., Erlendsson, Ö., McDermott, K., Petersen, U.K., 2016b. Moho and basement depth in the NE Atlantic Ocean based on seismic refraction data and receiver functions. In: Peron-Pinvidic, G., Hopper, J.R., Stoker, M., Gaina, C., Funck, T., Arting, U., Doornenbal, J.C. (Eds.), Geological Society. Special Publications, London.

Gabrielsen, R.H., Fossen, H., Faleide, J.I., Hurich, C.A., 2015. Mega-scale Moho relief and the structure of the lithosphere on the eastern flank of the Viking Graben, offshore southwestern Norway. Tectonics 34, 803–819.

Gaina, C., 2014. Plate reconstructions and regional kinematics. In: Hopper, J.R., Funck, T., Stoker, M., Árting, U., Peron-Pinvidic, G., Doornenbal, J.C., Gaina, C. (Eds.), Tectonostratigraphic Atlas of the North-East Atlantic Region. GEUS, Copenhagen.

Gaina, C., Nasuti, A., Kimbell, G.S., Blischke, A., 2017. Break-up and seafloor spreading domains in the NE Atlantic. In: Peron-Pinvidic, G., Hopper, J.R., Stoker, M., Gaina, C., Funck, T., Arting, U., Doornenbal, J.C. (Eds.), Geological Society. Special Publications, London.

Geissler, W.H., Gaina, C., Hopper, J.R., Funck, T., Blischke, A., Arting, U., Horni, J.Á., Péron-Pinvidic, G., Abdelmalak, M.M., 2016. Seismic volcanostratigraphy of the NE Greenland continental margin. In: Peron-Pinvidic, G., Hopper, J.R., Stoker, M., Gaina, C., Funck, T., Arting, U., Doornenbal, J.C. (Eds.), Geological Society. Special Publications, London.

Gresseth, J., Osmundsen, P.T., Peron-Pinvidic, G., 2021. Detachment Faulting, Successive Incision and Controls on Supradetachment Basin Formation at the Mid-Norwegian Rifted Margin - the Frøya High Turtleback, EGU, Online.

Griffin, W.L., O'Reilly, S.Y., 1987a. Is the continental Moho the crust-mantle boundary? Geology 15, 241–244.

Griffin, W.L., O'Reilly, S.Y., 1987b. Is the continental Moho the crust-mantle boundary? Geology 15, 241–244.

Hopper, J.R., Funck, T., Stoker, M., Árting, U., Peron-Pinvidic, G., Doornenbal, J.C., Gaina, C., 2014. Tectonostratigraphic Atlas of the North-East Atlantic Region. GEUS, Copenhagen.

Klemperer, S.L., Hobbs, R.W., 1991. The BIRPS Atlas. Cambridge University Press, Cambridge, Deep seismic reflection profiles around the British Isles.

Lavier, L.L., Manatschal, G., 2006. A mechanism to thin the continental lithosphere at magma-poor margins. Nature 440, 324–328.

Lenhart, A., Jackson, C.A.-L., Bell, R.E., Duffy, O.B., Gawthorpe, R.L., Fossen, H., 2019. Structural architecture and composition of crystalline basement offshore West Norway. Lithosphere 11, 273–293.

Lundin, E.R., Doré, A.G., 1997. A tectonic model for the Norwegian passive margin with implications for the NE Atlantic: early cretaceous to break-up. J. Geol. Soc. 154, 545–550.

Manatschal, G., Lavier, L., Chenin, P., 2014. The role of inheritance in structuring hyperextended rift systems: some considerations based on observations and numerical modeling. Gondwana Res. 27, 140–164.

Mjelde, R., Digranes, P., Shimamura, H., Shiobara, H., Kodaira, S., Brekke, H., Egebjerg, T., Sorenes, N., Thorbjornsen, S., 1998. Crustal structure of the northern part of the Voring Basin, mid-Norway margin, from wide-angle seismic and gravity data. Tectonophysics 293, 175–205.

MONA-LISA-working-group, 1997. MONA LISA — deep seismic investigations of the lithosphere in the southeastern North Sea. Tectonophysics 269, 1–19.

Mooney, W., 1992. Multigeneric origin of crustal reflectivity: a review of seismic reflection profiling of the continental lower crust and Moho. Continent. Lower Crust 45–79.

Muñoz-Barrera, J.M., Rotevatn, A., Gawthorpe, R.L., Henstra, G.A., Kristensen, T.B., 2020. The role of structural inheritance in the development of high-displacement crustal faults in the necking domain of rifted margins: the Klakk Fault complex, Frøya High, offshore mid-Norway. J. Struct. Geol. 140, 104163.

Naliboff, J.B., Buiter, S.J.H., Péron-Pinvidic, G., Osmundsen, P.T., Tetreault, J., 2017. Complex fault interaction controls continental rifting. Nat. Commun. 8, 1179.

Osmundsen, P.T., Ebbing, J., 2008. Styles of extension offshore mid-Norway and implications for mechanisms of crustal thinning at passive margins. Tectonics 27.

Osmundsen, P.T., Redfield, T., 2011. Crustal taper and topography at passive continental margins. Terra Nova 23, 349–361.

Osmundsen, P.T., Sommaruga, A., Skilbrei, J.R., Olesen, O., 2002. Deep structure of the Mid Norway rifted margin. Nor. J. Geol. 82, 205–224.

Osmundsen, P.T., Péron-Pinvidic, G., Bunkholt, H., 2020. Rifting of collapsed orogens: successive incision of continental crust in the proximal margin offshore Norway. Tectonics e2020TC006283.

Peron-Pinvidic, G., Åkermoen, T., 2020. MCG's Regional Deep Imaging Project: Norwegian Sea 2019. GeoExpro 17.

Peron-Pinvidic, G., Osmundsen, P.T., 2016. Architecture of the distal and outer domains of the mid-Norwegian Vøring rifted margin: insights from the Rån Ridge system. Mar. Pet. Geol. 77, 280–299.

Peron-Pinvidic, G., Osmundsen, P.T., 2018. The Mid Norwegian - NE Greenland conjugate margins: Rifting evolution, margin segmentation, and breakup. Mar. Pet. Geol. 98, 162–184.

Peron-Pinvidic, G., Osmundsen, P.T., 2020. From orogeny to rifting: insights from the Norwegian 'reactivation phase'. Sci. Rep. 10, 14860.
Peron-Pinvidic, G., Gernigon, L., Gaina, C., Ball, P., 2012. Insights from the Jan Mayen system in the Norwegian–Greenland sea—I. Mapping of a microcontinent. Geophys. J. Int. 191, 385–412.
Peron-Pinvidic, G., Manatschal, G., Osmundsen, P.T., 2013. Structural comparison of archetypal Atlantic rifted margins: a review of observations and concepts. Mar. Pet. Geol. 43, 21–47.
Peron-Pinvidic, G., Osmundsen, P.T., Bunkholt, H., 2020. The proximal domain of the Mid-Norwegian rifted margin: the Trøndelag Platform revisited. Tectonophysics 790, 228551.
Phillips, T.B., Jackson, C.A.L., Bell, R.E., Duffy, O.B., Fossen, H., 2016. Reactivation of intrabasement structures during rifting: A case study from offshore southern Norway. J. Struct. Geol. 91, 54–73.
Raum, T., Mjelde, R., Digranes, P., Shimamura, H., Shiobara, H., Kodaira, S., Haatvedt, G., Sørenes, N., Thorbjørnsen, T., 2002. Crustal structure of the southern part of the Vøring Basin, mid-Norway margin, from wide-angle seismic and gravity data. Tectonophysics 355, 99–126.
Ren, S., Faleide, J.I., Eldholm, O., Skogseid, J., Gradstein, F., 2003. Late Cretaceous-Paleocene tectonic development of the NW Voring Basin. Mar. Pet. Geol. 20, 177-206(130).
Reston, T.J., 2009. The structure, evolution and symmetry of the magma-poor rifted margins of the North and Central Atlantic: A synthesis. Tectonophysics 468, 6–27.
Reynisson, R.F., Ebbing, J., Lundin, E., Osmundsen, P.T., 2010. Properties and distribution of lower crustal bodies on the mid-Norwegian margin. In: Vining, B.A., Pickering, S.C. (Eds.), From Mature Basins to New Frontiers. Geological Society, London, pp. 843–854.
Savva, D., Pubellier, M., Franke, D., Chamot-Rooke, N., Meresse, F., Steuer, S., Auxietre, J.L., 2014. Different Expressions of Rifting on the South China Sea Margins. Marine and Petroleum Geology 58, Part B, pp. 579–598.
Singh, S.C., Hague, P.J., McCaughey, M., 1998. Study of the crystalline crust from a two-ship normal-incidence and wide-angle experiment. Tectonophysics 286, 79–91.
Snyder, D.B., Hobbs, R.W., 1999. The BIRPS Atlas II. A Second Decade of Deep Seismic Reflection Profiling. The Geological Society, London.
Tsikalas, F., Faleide, J.I., Eldholm, O., Antonio Blaich, O., 2012. 5 - the NE Atlantic conjugate margins. In: Bally, D.G.R.W. (Ed.), Regional Geology and Tectonics: Phanerozoic Passive Margins, Cratonic Basins and Global Tectonic Maps. Elsevier, Boston, pp. 140–201.
Wrona, T., Magee, C., Fossen, H., Gawthorpe, R.L., Bell, R.E., Jackson, C.A.-L., Faleide, J. I., 2019. 3-D seismic images of an extensive igneous sill in the lower crust. Geology 47, 729–733.